

Electronic Supplementary Information (ESI)

Multifunctional Low-Generation Dendrimer-Based Nanoprobe for Targeted Dual Mode MR/CT Imaging of Orthotopic Brain Gliomas

Xiaoying Xu,^{a, 1} Kang Liu,^{b, 1} Yue Wang,^{c, 1} Changchang Zhang,^a Menghan Shi,^a Peng Wang,^a
Linghong Shen,^d Jindong Xia,^{*c} Ling Ye,^{*b} Xiangyang Shi,^{*a} Mingwu Shen^{*a}

^a State Key Laboratory for Modification of Chemical Fibers and Polymer Materials, College
of Chemistry, Chemical Engineering and Biotechnology, Donghua University, Shanghai
201620, People's Republic of China

^b School of Chemical Biology and Pharmaceutical Sciences, Capital Medical University,
Beijing 100069, People's Republic of China

^c Department of Radiology, Shanghai Songjiang District Central Hospital, Shanghai 201600,
People's Republic of China

^d Department of Cardiology, Shanghai Chest Hospital, Shanghai Jiaotong University School
of Medicine, Shanghai 200030, People's Republic of China

* Corresponding author. E-mail: xiajd_21@163.com (J. Xia), lingye@ccmu.edu.cn (L. Ye),
xshi@dhu.edu.cn (X. Shi), and mwshen@dhu.edu.cn (M. Shen)

¹ Authors contributed equally to this work.

Experimental section

Materials

2,2'-(7-(2-((2,5-Dioxopyrrolidin-1-yl)oxy)-2-oxoethyl)-1,4,7-triazonane-1,4-diyl)diacetic acid (NOTA-NHS ester) was purchased from CheMatech (Dijon, France). N-Hydroxysuccinimide (NHS), 1-(3-dimethylaminopropyl)-3-ethylcarbodiimide hydrochloride (EDC), manganese acetate ($C_4H_6MnO_4 \cdot 4H_2O$) and sodium borohydride ($NaBH_4$) were from J&K Chemical Ltd. (Shanghai, China). Ethylenediamine core G2.NH₂ PAMAM dendrimers were acquired from Dendritech (Midland, MI). Thiolated cyclic arginine-glycine-aspartic (Arg-Gly-Asp, RGD) peptide (Mw = 690.93) was purchased from GenicBio (Shanghai, China). $HAuCl_4 \cdot 4H_2O$ was obtained from Sinopharm Chemical Reagent Co., Ltd. (Shanghai, China). PEG with maleimide group at one end and carboxyl group at the other end (MAL-PEG-COOH, Mw = 2000) and PEG monomethyl ether with carboxyl terminal group (*m*PEG-COOH, Mw = 2000) were supplied by Shanghai Yanyi Biotechnology Corporation (Shanghai, China). Dimethyl sulfoxide (DMSO) and all other chemicals and solvents were purchased from Sigma-Aldrich (St. Louis, MO) and used as received. C6 glioma cells (a rat C6 glioma cell line) were obtained from Institute of Biochemistry and Cell Biology, the Chinese Academy of Sciences (Shanghai, China). Dulbecco's modified Eagle medium (DMEM), fetal bovine serum (FBS), penicillin, and streptomycin were purchased from Hangzhou Jinuo Biomedical Technology (Hangzhou, China). Cell counting kit-8 (CCK-8) was supplied by 7Sea Pharmatech Co., Ltd. (Shanghai, China). Calcein-AM was obtained from KeyGEN BioTECH. Co., Ltd. (Nanjing, China). The water used in all experiments was purified using a Milli-Q Plus 185 water purification system (Millipore, Bedford, MA) and exhibited a resistivity greater than 18.2 MΩ·cm. Cellulose dialysis membranes possessing molecular weight cut-offs (MWCOs) of 1000 and 3000 were acquired from Shanghai Yuanye Biotechnology Corporation (Shanghai, China).

Synthesis of the Au-Mn DENPs

MAL-PEG-COOH (90.0 mg) dissolved in 4 mL of DMSO was mixed with equal molar equiv. of RGD peptide (32 mg) dissolved in 3 mL of DMSO under stirring for 24 h. The product of RGD-PEG-COOH was got after dialysis and lyophilization according to the literature.¹ After that, the raw product of G2-NOTA was obtained through the reaction of G2.NH₂ (30.0 mg, dissolved in 3 mL of DMSO) with 6 molar equiv. of NOTA-NHS ester (36.5 mg, dissolved in 3 mL DMSO) under stirring for 24 h. Then 5 molar equiv. of RGD-PEG-COOH (95 mg) or equal molar equiv. of *m*PEG-COOH (100 mg) preactivated *via* EDC (92.0 mg) and NHS (55.0 mg) in 8 mL of DMSO was added to the solution of the raw product of G2-NOTA under stirring for 3 days. The mixture was dialyzed against water (9 times, 2 L) for 3 days *via* the cellulose dialysis membrane with an MWCO of 3000, followed by lyophilization to get the product of G2-NOTA-PEG-RGD or G2-NOTA-*m*PEG dendrimers. Then, the G2-NOTA-PEG-RGD dendrimers were used as templates to synthesize Au NPs through NaBH₄ reduction with the dendrimer/gold salt molar ratio of 1/6. Next, after dialysis and lyophilization, the obtained RGD-Au DENPs were mixed with 4 molar equiv. of C₄H₆MnO₄·4H₂O in weakly acidic water solution for 24 h, followed by dialysis against water for 3 days (9 times, 2 L) and lyophilization to obtain the product of RGD-Au-Mn DENPs. The non-targeted Au-Mn DENPs without RGD were also acquired under the same conditions.

Characterization techniques

¹H NMR spectra were recorded on a Bruker AV400 nuclear magnetic resonance spectrometer (Karlsruhe, Germany). D₂O was used as a solvent to dissolve samples before measurements. Zeta potential and dynamic light scattering (DLS) were carried out using a Malvern Zetasizer Nano ZS model ZEN3600 (Worcestershire, U.K.) coupled with a standard 633 nm laser. To evaluate the colloidal stability of Au-Mn NPs, the hydrodynamic sizes of the Au-Mn NPs were also measured after they were stored at different time periods (0, 1, 3, 5 and 7 days, respectively). Leeman Prodigy inductively coupled plasma-optical emission

spectroscopy (ICP-OES, Hudson, NH) was used to measure the Au and Mn concentrations of the particle suspension. The stability of Au-Mn NPs was also evaluated by determining the leakage of Mn(II) ions from the Au-Mn NPs. In brief, the synthesized Au-Mn NPs were dispersed into PBS ($[Mn] = 0.4 \text{ mM}$) and stored at 37°C for 1, 3, and 7 days. At each time point, the Au-Mn NPs suspension was centrifuged (18000 rpm, 10 min) to acquire the supernatants. The Mn contents in the supernatants were measured by ICP-OES. Finally, the relative Mn contents (% of original) in the supernatants were calculated to evaluate the Mn leakage. UV-vis spectroscopy was implemented using a Lambda 25 UV-vis spectrophotometer (PerkinElmer, Boston, MA) and samples were dissolved in water before UV-vis spectral measurements. Transmission electron microscopy (TEM) imaging was executed using a JEOL 2010F analytical electron microscope (JEOL, Tokyo, Japan) at an operating voltage of 200 kV. TEM samples were prepared by dropping an ethanol particle suspension (1 mg/mL) onto a carbon-coated copper grid, and the ethanol suspension was air-dried before measurements. The size distribution histograms of the particles were measured using ImageJ software (<http://www.rsb.info.nih.gov/ij/download.html>). For each sample, 200 NPs were randomly selected to analyze the size distribution. The T_1 relaxation times of samples were measured by a 0.5 T NMI20-Analyst NMR analyzing and imaging system (Shanghai Niumag Corporation, Shanghai, China) with the following parameters: point resolution = $156 \text{ mm} \times 156 \text{ mm}$; section thickness = 0.6 mm ; $TR = 4000 \text{ ms}$; $TE = 60 \text{ ms}$; and number of excitations = 1. The samples were diluted in water with Mn concentration in a range of $0.1\text{-}1.6 \text{ mM}$. The r_1 relaxivity was calculated by linearly fitting the inverse T_1 relaxation time ($1/T_1$) as a function of Mn concentration.² CT scans were performed using a clinical Brilliance 64-slice CT imaging system (Philips Healthcare, Andover, MA) with 120 kV, 200 mA, and a slice thickness of 1.5 mm to characterize the X-ray attenuation property of the samples. RGD-Au-Mn DENPs solutions and Omnipaque ($300 \text{ mg}\cdot\text{mL}^{-1}$, used as control group, GE Healthcare, Princeton, NJ) with Au or iodine concentration in a range of $0.005\text{-}0.04 \text{ M}$ were collected in 1.5-mL Eppendorf

tubes. Evaluation of X-ray attenuation property was carried out by loading the digital CT images in a standard display program and then selecting a uniform round region on the resultant CT images for each sample. The CT contrast enhancement was evaluated through testing the value of Hounsfield unit (HU) for each concentration of the RGD-Au-Mn DENPs or Omnipaque.³

***In vitro* cytotoxicity assay, cell morphology observation, and cellular uptake assay**

C6 glioma cells were regularly cultured and passaged in DMEM supplemented with 10% fetal bovine serum, 100 U·mL⁻¹ penicillin, and 100 µg·mL⁻¹ streptomycin, in humidified air containing 5% CO₂ at 37 °C.

To assess the cytotoxicity of the RGD-Au-Mn and non-targeted Au-Mn DENPs, C6 glioma cells were seeded into a 96-well culture plate at a density of 1×10^4 cells per well with 200 µL DMEM for 24 h. Then the medium was substituted with fresh medium containing RGD-Au-Mn DENPs or non-targeted Au-Mn DENPs with different Mn concentrations (25, 50, 100, 200, and 400 µM, respectively), followed by incubation for 24 h (PBS as a control). Then, DMEM containing 10% CCK-8 solution (100 µL) was added into each well before incubation for an additional 4 h. The absorbance of each well was recorded using a Thermo Scientific Multiskan MK3 ELISA reader (Thermo Scientific, Waltham, MA) at 450 nm. For each sample, mean and standard deviation (SD) of six parallel wells were recorded.

To further confirm the cytocompatibility of the RGD-Au-Mn or non-targeted Au-Mn DENPs, C6 glioma cells were treated with different materials at various Mn concentrations (25, 50, 100, 200, and 400 µM, respectively) for 24 h. The cells were rinsed three times with PBS and added with 100 µL DMEM containing 0.125% calcein-AM. After staining for 15 min, the cells were rinsed three times with PBS and observed by Zeiss Axio Vert. A1 inverted fluorescence microscope (Carl Zeiss, Jena, Germany) with 100× magnification.

ICP-OES analysis was performed to quantify the specific cellular uptake⁴ of the RGD-Au-Mn DENPs in C6 glioma cells. Briefly, 2×10^5 cells were seeded into 12-well culture plates

for 24 h to bring the cells to confluence. After that, the medium was replaced with fresh medium containing RGD-Au-Mn or non-targeted Au-Mn DENPs with different Mn concentrations (25, 50, 100, 200, and 400 μ M, respectively), followed by incubation for 4 h (PBS as a control). Next, the cells were rinsed three times with PBS, trypsinized, and centrifuged to remove the supernatant. Thereafter, all cells were digested by *aqua regia* (nitric acid/hydrochloric acid, v/v = 1: 3) for 10 min, and the solution was diluted before subsequent ICP-OES measurements of Mn concentration.

MR/CT imaging of an orthotopic mouse brain glioma model

All animal experiments were carried out following the protocols approved by the Ethical Committee of Capital Medical University and Shanghai Songjiang District Central Hospital, and according to the policy of the National Ministry of Health. ICR mice were purchased from the Shanghai SLAC Laboratory Animal Center (Shanghai, China).

ICR mice were anesthetized with 6% chloral hydrate (0.10 mL/20 g) and placed in a stereotactic frame. A burr hole was drilled into the skull (1.0 mm anterior and 2.0 mm lateral to the bregma). Approximately 5×10^5 C6 glioma cells (suspended in a total volume of 5 μ L PBS) were injected into the burr hole. When the tumors reached 1.5–1.8 mm in diameter, MR and CT imaging was performed.⁵ Each ICR mouse was anesthetized with 6% chloral hydrate (0.10 mL/20 g), and then the RGD-Au-Mn or non-targeted Au-Mn DENPs were intravenously injected into each mouse *via* the tail vein ([Mn] = 400 μ g, [Au] = 0.05 M, in 150 μ L PBS). Subsequently, each ICR mouse was placed in an anesthetic chamber confined in a gantry and maintained with 2% isoflurane. Eventually, MR scanning of the mice was carried out using a 1.5 T Signa HDxt superconductor MR system (GE Medical Systems, Milwaukee, WI). The T₁-weighted MR images were recorded with the following parameters: TR = 1959 ms; TE = 16.1 ms; point resolution = 256 mm \times 256 mm; section thickness = 1 mm; FOV = 80 \times 80 mm; and number of excitations = 1. CT scanning of the mice was carried out using a clinical Brilliance

64-slice CT imaging system (Philips Healthcare, Andover, MA) with 80 kV, 450 mA, and a slice thickness of 45 mm.

In vivo biodistribution

To assess the biodistribution of the RGD-Au-Mn or non-targeted Au-Mn DENPs, the tumor-bearing ICR mice were intravenously injected with the particles ([Au] = 0.05 M, in 150 μ L PBS for each mouse). The mice were euthanized at 45 min, 12 h and 24 h postinjection and the major organs including the heart, liver, spleen, lung, kidney and brain were extracted and weighed. The organs were cut into small pieces and digested by *aqua regia* for 7 days before ICP-OES quantification of the Au element. For comparison, tumor-bearing mice injected with PBS (150 μ L for each mouse) were used as control.

Histological examinations

Healthy ICR mice were intravenously injected with PBS containing RGD-Au-Mn or non-targeted Au-Mn DENPs ([Au] = 0.05 M, in 150 μ L PBS for each mouse) through the tail vein (PBS was used as control). After 3 weeks treatment, the mice were anesthetized and sacrificed, and their liver, lung, spleen, heart, and kidney were harvested. Then these organs were fixed, embedded, sectioned, and stained with H&E according to protocols reported in the literature.⁶ Finally, the organ sections were observed under Leica DM IL LED inverted phase contrast microscope (Wetzlar, Germany) at a magnification of $100\times$ for each sample.

Statistical analysis

One-way ANOVA statistical analysis was performed to evaluate the significance of the experimental data. A value of 0.05 was selected as the significance level, and the data were indicated with (*) for $p < 0.05$, (**) for $p < 0.01$, and (***) for $p < 0.001$, respectively.

Table S1. Zeta potentials and hydrodynamic sizes of the non-targeted Au-Mn and RGD-Au-Mn DENPs. Data are provided as mean \pm SD (n = 3).

Samples	Zeta potential (mV)	Hydrodynamic size	Polydispersity index
		(nm)	(PDI)
Non-targeted	$+3.3 \pm 0.45$	58.0 ± 4.88	0.41 ± 0.026
Targeted	$+6.2 \pm 0.04$	86.6 ± 3.21	0.25 ± 0.047

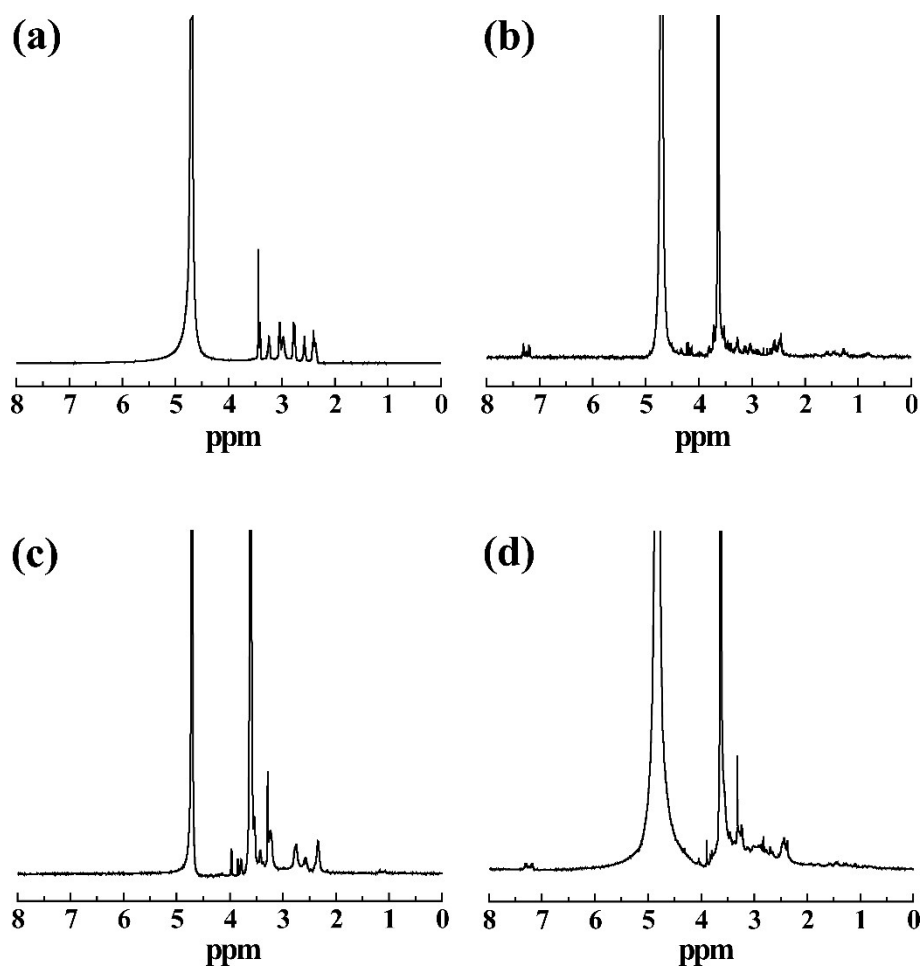


Figure S1. ^1H NMR spectra of G2-NOTA (a), RGD-PEG-COOH (b), G2-NOTA-*m*PEG (c) and G2-NOTA-PEG-RGD (d).

Through ^1H NMR integration, we were able to estimate the number of RGD bound to each PEG to be 0.8, and those of NOTA and RGD-PEG-COOH (or *m*PEG-COOH) to be 3.6 and 7.5 (or 8.2), respectively.

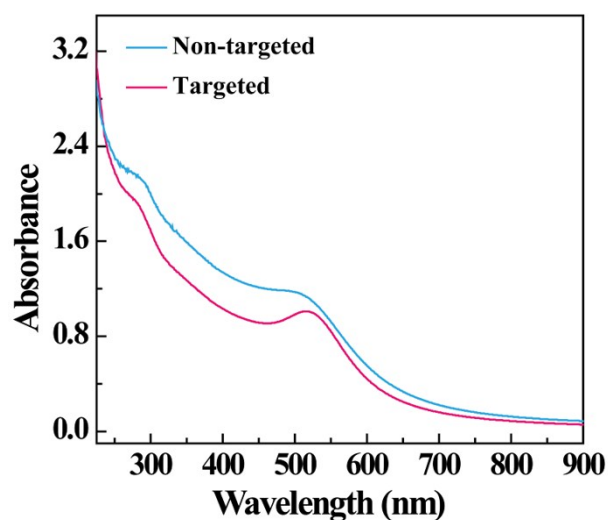


Figure S2. UV-vis spectra of non-targeted Au-Mn and RGD-Au-Mn DENPs.

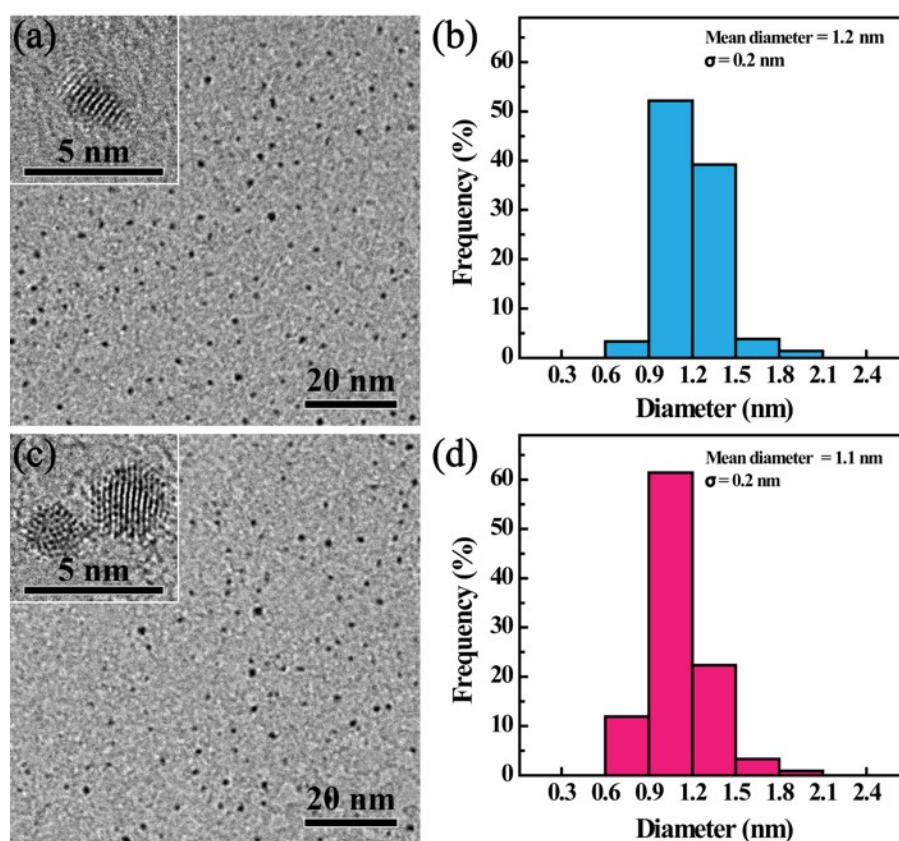


Figure S3. TEM images and size distribution histogram of the non-targeted Au-Mn (a, b) and RGD-Au-Mn DENPs (c, d), respectively. Insets of (a) and (c) show the high-resolution TEM image of the corresponding DENPs.

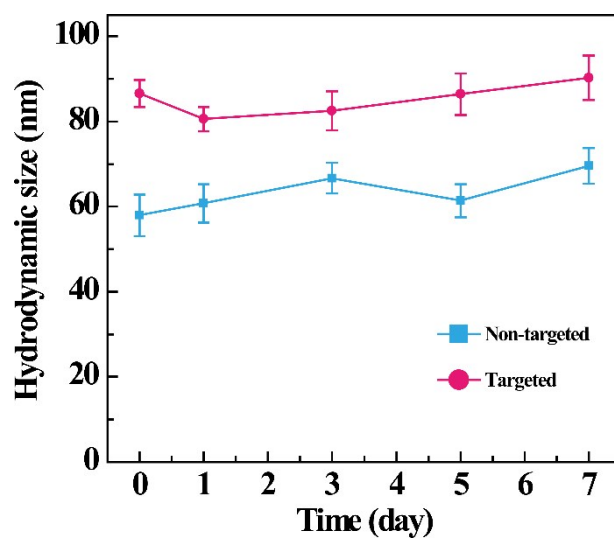


Figure S4. Hydrodynamic size of the Au-Mn NPs in aqueous solution at various storage time periods.

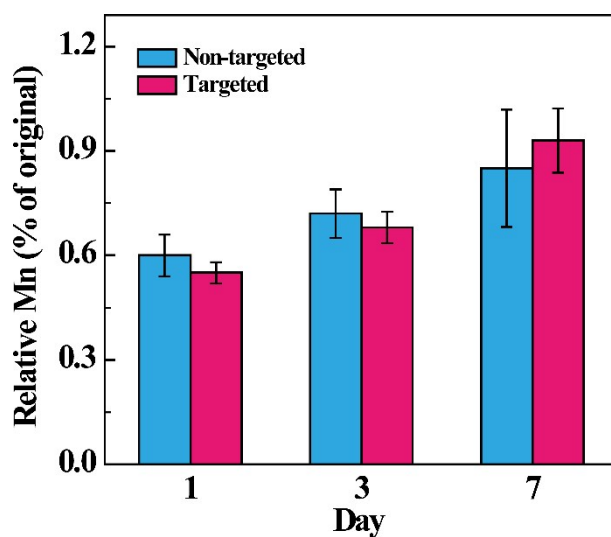


Figure S5. The relative Mn contents (% of original) in the supernatants of Au-Mn NPs (Mn = 0.4 mM) after stored at 37 °C for 1, 3 and 7 days, respectively, followed by centrifugation.

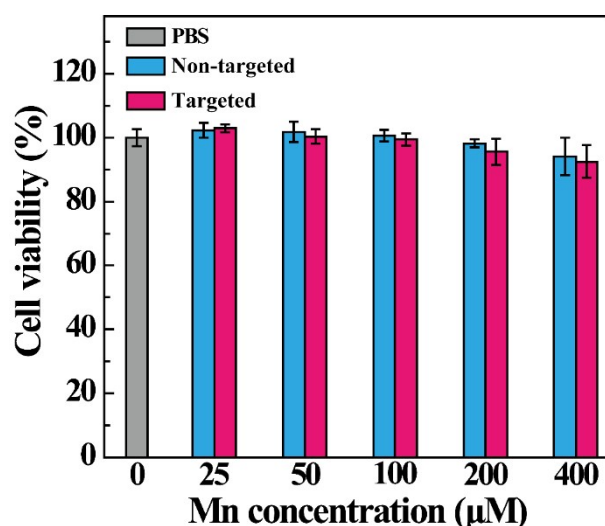


Figure S6. CCK-8 viability assay of C6 glioma cells ($n = 6$ for each Au concentration) after treated with the non-targeted Au-Mn and RGD-Au-Mn DENPs for 24 h at the Mn concentrations of 0, 25, 50, 100, 200 and 400 μM , respectively.

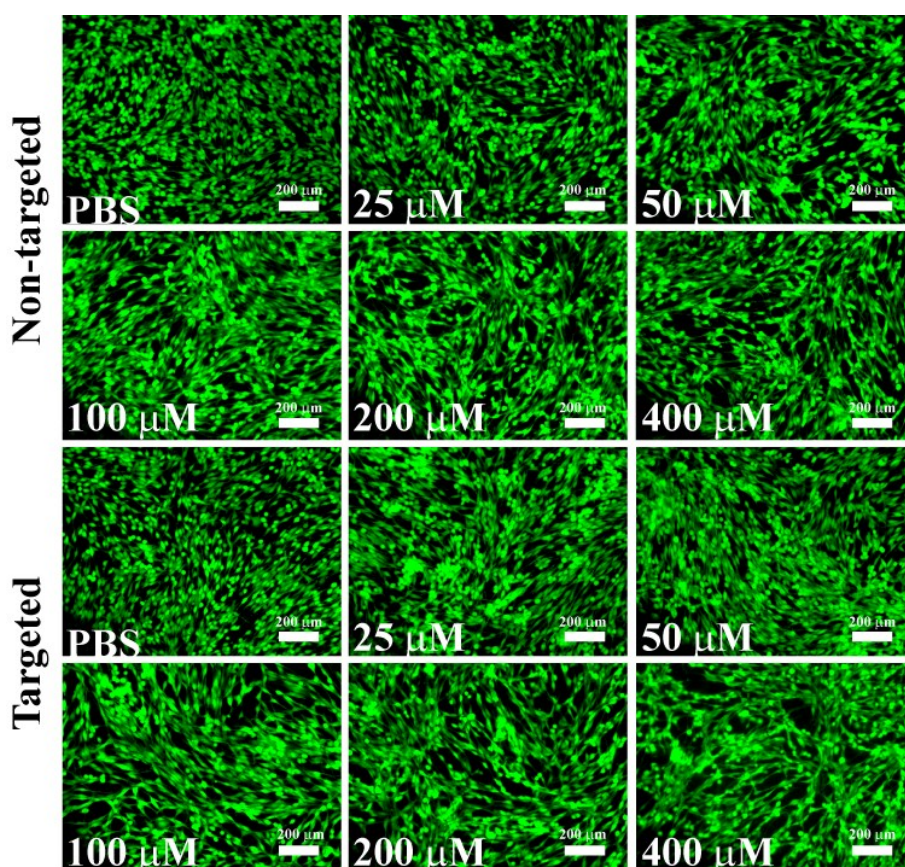


Figure S7. Fluorescence microscopic images of C6 glioma cells stained with calcein-AM after treatment with the non-targeted Au-Mn and RGD-Au-Mn DENPs for 24 h at the Mn concentration of 0, 25, 50, 100, 200 and 400 μM , respectively.

Cell morphology was observed after the cells were treated with either non-targeted Au-Mn and RGD-Au-Mn DENPs. Calcein-AM staining of cells reveals that in comparison with the

PBS control, the addition of both non-targeted Au-Mn and RGD-Au-Mn DENPs at the same concentrations does not seem to cause any apparent changes of cell morphology, further confirminbg the excellent cytocompatibility of the as-prepared Au-Mn DENPs.

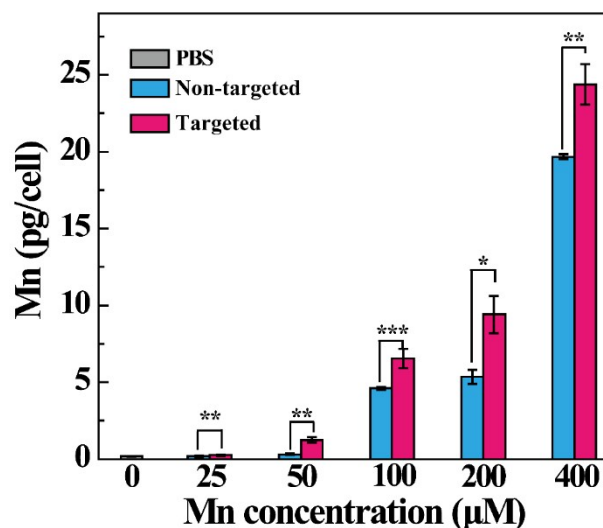


Figure S8. Cellular uptake of Mn in C6 glioma cells treated with the non-targeted Au-Mn and RGD-Au-Mn DENPs for 4 h at the Mn concentration of 0, 25, 50, 100, 200 and 400 μM, respectively (n = 3).

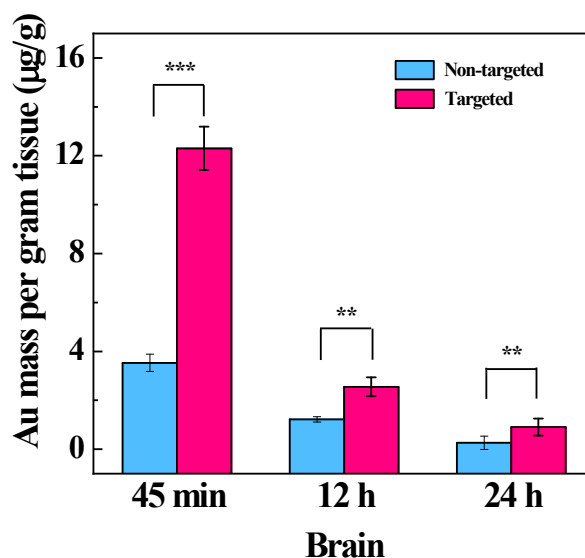


Figure S9. Biodistribution of Au element in the brain. The data were recorded from the whole brain of tumor-bearing mice taken at 45 min, 12 h and 24 h postinjection of the non-targeted Au-Mn and RGD-Au-Mn DENPs ([Mn] = 400 μg, [Au] = 0.05 M, in 150 μL PBS, for each mouse, n = 3).

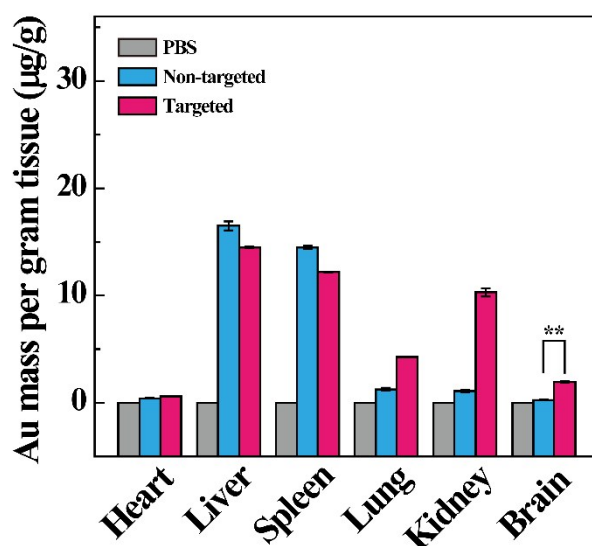


Figure S10. Biodistribution of Au element in the brain and the major organs of the mice including the heart, liver, spleen, lung and kidney. The data were recorded from the whole brain of tumor-bearing mice taken at 24 h postinjection of the non-targeted Au-Mn and RGD-Au-Mn DENPs ([Mn] = 400 μ g, [Au] = 0.05 M, in 150 μ L PBS, for each mouse, n =3).

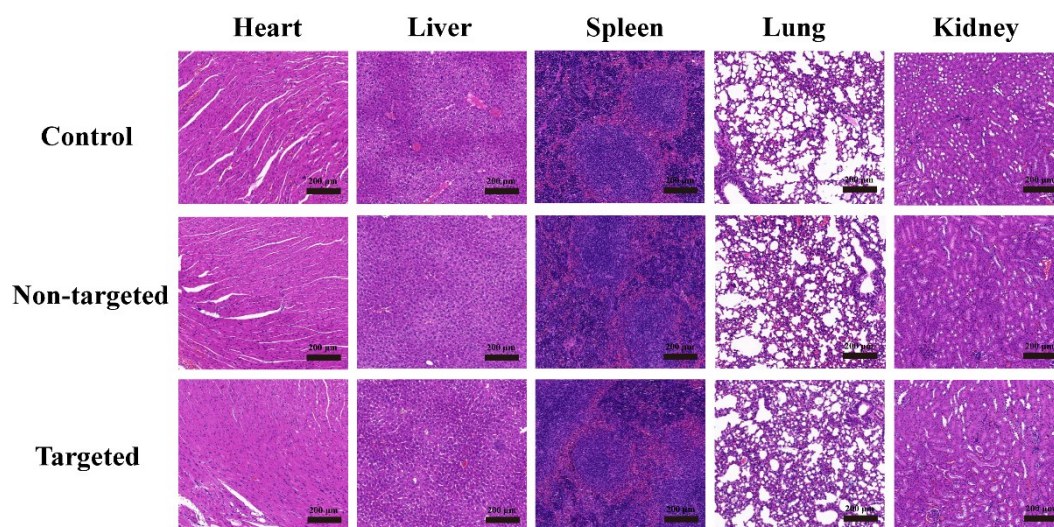


Figure S11. Histological changes in the heart, liver, spleen, lung and kidney of the mice at 3 weeks postinjection of the non-targeted Au-Mn and RGD-Au-Mn DENPs ([Mn] = 400 μ g, [Au] = 0.05 M, in 150 μ L PBS for each mouse). Mice injected with PBS (150 μ L for each mouse) were used as control. The organ sections were H&E stained and observed under Leica DM IL LED inverted phase contrast microscope at a magnification of 100 \times (the scale bar in each panel indicates 200 μ m).

The potential long-term toxicity of the Au-Mn DENPs was further assessed by H&E staining of the main organ slices of mice at 3 weeks postinjection (Figure S11). No obvious lesion, inflammation, or tissue damage was observed for all the main organs, which is similar to the PBS control. Hence, both the targeted and the non-targeted Au-Mn DENPs show good biosafety profile in the long term.

References

1. X. Y. Xu, L. Z. Zhao, X. Li, P. Wang, J. H. Zhao, X. Y. Shi and M. W. Shen, *Biomater. Sci.*, 2017, **5**, 2393-2397.
2. P. Wang, J. Yang, B. Q. Zhou, Y. Hu, L. X. Xing, F. L. Xu, M. W. Shen, G. X. Zhang and X. Y. Shi, *ACS Appl. Mater. Interfaces*, 2017, **9**, 47-53.
3. Y. Dou, Y. Guo, X. Li, X. Li, S. Wang, L. Wang, G. Lv, X. Zhang, H. Wang, X. Gong and J. Chang, *ACS Nano*, 2016, **10**, 2536-2548.
4. S. Behzadi, V. Serpooshan, W. Tao, M. A. Hamaly, M. Y. Alkawareek, E. C. Dreaden, D. Brown, A. M. Alkilany, O. C. Farokhzad and M. Mahmoudi, *Chem Soc Rev*, 2017, **46**, 4218-4244.
5. K. Liu, X. Shi, T. J. Wang, P. H. Ai, W. Gu and L. Ye, *J. Colloid Interface Sci.*, 2017, **485**, 25-31.
6. S. R. Bhattarai, P. J. Derry, K. Aziz, P. K. Singh, A. M. Khoo, A. S. Chadha, A. Liopo, E. R. Zubarev and S. Krishnan, *Nanoscale*, 2017, **9**, 5085-5093.